

PCCP

Accepted Manuscript



This is an *Accepted Manuscript*, which has been through the Royal Society of Chemistry peer review process and has been accepted for publication.

Accepted Manuscripts are published online shortly after acceptance, before technical editing, formatting and proof reading. Using this free service, authors can make their results available to the community, in citable form, before we publish the edited article. We will replace this *Accepted Manuscript* with the edited and formatted *Advance Article* as soon as it is available.

You can find more information about *Accepted Manuscripts* in the [Information for Authors](#).

Please note that technical editing may introduce minor changes to the text and/or graphics, which may alter content. The journal's standard [Terms & Conditions](#) and the [Ethical guidelines](#) still apply. In no event shall the Royal Society of Chemistry be held responsible for any errors or omissions in this *Accepted Manuscript* or any consequences arising from the use of any information it contains.

Effect of acetone on the dynamics of temporal oscillations and waves in the ruthenium-catalyzed Belousov-Zhabotinsky reaction

Titikan Somboon,^a Prapin Wilairat,^a Stefan C. Müller^b and On-Uma Kheowan^{*a}

Received Xth XXXXXXXXXXXX 20XX, Accepted Xth XXXXXXXXXXXX 20XX

First published on the web Xth XXXXXXXXXXXX 200X

DOI: 10.1039/b000000x

The effect of acetone on temporal oscillations and spatio-temporal patterns occurring in the ruthenium-catalyzed Belousov-Zhabotinsky (BZ) reaction was investigated in a closed batch system. The periods of temporal oscillations and waves significantly decrease with increasing acetone concentration. At low concentrations of acetone (0.01–0.05 M), regular wave patterns are observed with prolonged lifetime of both temporal oscillations and waves. However, for higher concentrations (0.10–1.00 M acetone), the duration of the oscillatory phase is shortened and irregular patterns are formed. The photosensitivity of waves of the Ru(bpy)₃²⁺-catalyzed BZ reaction remains the same for all acetone concentrations. The results are discussed in terms of proposed reaction mechanism.

1 Introduction

^aDepartment of Chemistry, Faculty of Science, Mahidol University, Rama 6 Road, Bangkok 10400, Thailand. Corresponding author e-mail: on-uma.khe@mahidol.ac.th

^bInstitut für Experimentelle Physik, Otto-von-Guericke-Universität,

The main feature of the BZ reaction is the oxidation of an organic compound, such as malonic acid, by bromate under acidic conditions in the presence of a metal ion catalyst, e.g., ruthenium.^{1–3} This reaction can exhibit both temporal oscillations and spatial pattern formation in the form of chemical waves, which occur when the system is far from its thermodynamic equilibrium state.^{4,5} The typical reactor employed for studying the chemical oscillations is a closed batch reactor, in which all of the reagents are mixed under continuous stirring without addition of reagents or removal of the reacting solution.⁴ Since the reactants are consumed, the system has a limited lifetime of the oscillations. The reaction lifetime is also limited by the accumulated Br₂, which is known to inhibit the BZ reaction.⁴ Br₂ can be removed by stirring the reaction solution or by bubbling an inert carrier gas.⁶ Another method to remove the Br₂ is by addition of ketones, such as acetone, methyl ethyl ketone, methyl propyl ketone, or methyl isobutyl ketone, to the BZ reaction.^{7–9}

Acetone is one of the most widely used compounds as a Br₂ remover for the BZ reaction. For example, it was employed in the BZ system with an organic compound that is not readily brominated, i.e., oxalic acid.¹⁰ In such systems, the amount of Br[–] is controlled by Br₂ hydrolysis. In the original BZ reaction employing malonic acid, increase of the acetone concentration extended the time for reaching the crucial concentration of bromomalonic acid, leading to enhancement of the induction period.^{7–9} Less malonic acid reacts with Br₂ with the addition of acetone, which results in an increase in the number

Universitätsplatz 2, D-39106, Magdeburg, Germany.

of oscillations. However, the oscillation period remained the same for acetone concentration in the range 0.00-0.059 M.⁷⁻⁹

Acetone was also employed for removal of Br₂ in the bromate-hypophosphite-acetone-dual catalyst system.^{11,12} In this system, hypophosphite was used instead of malonic acid to avoid the generation of CO₂ bubbles, which interfered with the observation of waves. The main catalyst used was Mn(II) with either Ru(II) complex, cerium(IV) or ferroin as the second catalyst.¹² Ru(bpy)₃SO₄ was employed as a secondary catalyst in the photosensitive system. The system gave long lasting oscillations and waves (more than 6 hours).¹¹ The system is ideally suited for studying pattern evolution, since it produces long duration of patterns for more than 6 hours, no accumulation of gas, and photosensitivity.^{11,12} A disadvantage of the system, however, is the relatively long wavelength of waves, which prevents the development of large numbers of waves when Petri dish is employed.¹²

Although many BZ systems with acetone have been investigated previously, the range of acetone concentration was relatively small (0.00-0.12 M).⁸⁻¹² In this research this range is extended to 1.00 M to observe the effect of such large of acetone on the period of both temporal oscillations and waves. Here we employ only one catalyst, i.e., the light sensitive Ru(bpy)₃²⁺, which is simpler than the dual catalyzed BZ system.¹² We are interested in the dynamic parameters, such as period and lifetime and also the photosensitivity of spatio-temporal patterns, which is important in the study and control of wave dynamics in the long term. The experimental results are discussed based on the concepts of chemical kinetics and the FKN mech-

anism.^{1-3,8-10}

2 Experimental section

2.1 Temporal oscillations

The temporal oscillations were studied under closed batch condition. The starting reagents were 0.05 M sodium bromate (Fluka 99%, Switzerland), 0.20 M malonic acid (Fluka 98%, Switzerland), 0.50 M sulfuric acid (Fluka 96%, Switzerland) and 1.0×10^{-4} M tris(bipyridine)ruthenium(II) sulfate. Ru(bpy)₃SO₄ was obtained by precipitation from Ru(bpy)₃Cl₂ (Alfa Aesar 98%, USA).^{13,14} Concentrations of acetone (Emure 98%, Germany) were 0.00, 0.01, 0.05, 0.10, 0.50 and 1.00 M, respectively. Vapor pressure of acetone at 25°C is 0.282 atm.¹⁵ The final volume of the BZ reagents was 50 ml, which was transferred into a beaker (100 ml) wrapped with aluminium foil to protect from ambient light. The beaker was capped with a cork plug (see EIS 1). The volume of space over the BZ solution is 25 ml. The beaker was placed in a thermostated water jacket, maintained at $25.0 \pm 0.2^\circ\text{C}$. The evaporation of acetone was estimated from Raoult's Law and the ideal gas law. We found that the calculated evaporation was about 0.01% of total acetone, which is relatively small. Therefore, under this physically closed system, the evaporation would not lead to any significant loss of acetone.

The solution was stirred with a magnetic bar at a constant rate of 300 rpm. The temporal oscillations were simultaneously followed with a combination platinum ring indicator electrode with a silver/silver chloride reference electrode (InLab Redox

Pro, Mettler Toledo, Switzerland) and a combination bromide ion selective electrode (HI 4102 bromide combination electrode with a silver/silver chloride reference electrode, Hanna Instrument, Japan). The internal double junction filling solution of both reference electrodes was 1 M KNO_3 to avoid chloride ions that can inhibit the oscillations.^{16,17} The electrodes were connected to a dual channel pH meter (HI 4212, Hanna Instrument, Japan). The pH meter was connected to a computer *via* USB connector. The experimental data were recorded using the HI 92000 Windows compatible software.

2.2 Spatio-temporal patterns

In the study of the spatio-temporal patterns, the catalyst $\text{Ru}(\text{bpy})_3\text{SO}_4$ was immobilized in a silica-gel matrix to avoid hydrodynamic perturbations.¹⁸ The mixture of $\text{Ru}(\text{bpy})_3\text{SO}_4$, H_2SO_4 and H_2O was added drop wise, under continuous stirring, to 2 ml of waterglass solution. Then 3 ml of the solution was pipetted into a Petri dish (6.99 ± 0.01 cm). After gelation, the gel was neutralized by covering with 6 ml of 0.1 M H_2SO_4 solution for 30 minutes and subsequently washed 3 times with H_2O . It was kept covered with H_2O before starting the experiment to prevent desiccation. The thickness of the gel was 0.61 ± 0.02 mm (measured with a micrometer). The BZ solution (10 ml), consisting of NaBrO_3 , malonic acid, H_2SO_4 , and H_2O was poured on top of the gel. The volume of air space over the BZ solution is 21 ml and the calculated evaporation of acetone is about 0.03%. The concentrations, after pseudo-equilibrium between liquid and gel, were 0.05 M NaBrO_3 , 0.20 M malonic acid, 5×10^{-4} M $\text{Ru}(\text{bpy})_3\text{SO}_4$, and 0.50 M H_2SO_4 .

The acetone concentrations were the same as for the study of the temporal oscillations in Section 2.1. The temperature was controlled by using a temperature control unit, in which water from a thermostat was circulated through a coil of copper tubing. The temperature was maintained at $25.0 \pm 0.2^\circ\text{C}$. Chemical waves were observed in transmitted light by a CCD camera.^{13,14} The illuminating light was filtered by a bandpass filter (310-530 nm) and the illumination intensity was measured by using a photometer (Newport, 1815-C) placed at the location of the Petri dish. The ambient (dark) light intensity was $0.12 \mu\text{W}/\text{cm}^2$. Normally, the light intensity was fixed at $47.0 \pm 0.5 \mu\text{W}/\text{cm}^2$. However, in one experiment the light intensities were varied at 10.3, 30.6, 50.9, and $78.2 \mu\text{W}/\text{cm}^2$, respectively, when investigating the effect of illumination for different concentrations of acetone.

3 Results

3.1 Temporal oscillations

When the BZ chemicals are mixed, the color of the solution alternately changes from orange to green (reduced to oxidized state of the $\text{Ru}(\text{bpy})_3^{2+}$ catalyst); and temporal oscillations are observed for the potentials of both the Pt electrode and the bromide selective electrode respectively. Typical temporal traces of the oscillations of the BZ reaction without acetone observed with these two electrodes are shown in Figs. 1a and 1b, respectively. Initially, the minimum values of the Pt potential decreases and then after 30-40 min remain almost constant. The time when the minimum value starts to be almost constant is

defined as t_b . After this time, the system shows regular oscillations of potentials at the Pt and bromide selective electrodes (see the inset of Fig.1). The interval between data points in the inset is 1 s. The amplitude of temporal oscillations decreases with time and the system finally reaches its equilibrium, when the oscillations ceases.

The period of the temporal oscillations (T_{10}), oscillation lifetime (L_{10}), and oscillation number (N_{10}) can be determined from the potential data of the Pt electrode. T_{10} , which is the main dynamical parameter of oscillations, is defined as the time interval between two consecutive peaks. The threshold value of $0.6 \times (V_{max} - V_{min}) + V_{min}$ is employed for the peak potential, where V_{max} and V_{min} are the maximum potential and minimum potential of each peak. Because T_{10} decreases with time, the characteristic value of T_{10} is averaged after t_b , as established in the time interval 45-55 min. For example, T_{10} of the experimental data in Fig. 1 over the time interval 45-55 min is 63 ± 1 s. L_{10} is defined as the time interval between the start and the cessation of oscillations. The oscillations are considered to cease, when the amplitude of the potential is less than 2% of the amplitude at t_b . L_{10} of the recipe without acetone in Fig. 1 is 491 ± 13 min. However, since T_{10} is not constant in time, T_{10} and L_{10} are not sufficient to characterize the overall dynamics of oscillations. Another parameter that describes the oscillation dynamics is N_{10} , which is the number of oscillation peaks counted from the start to the end of oscillations. N_{10} for the system without acetone is 756 ± 21 (mean and range of two experiments).

The effect of acetone on the temporal oscillations of the bro-

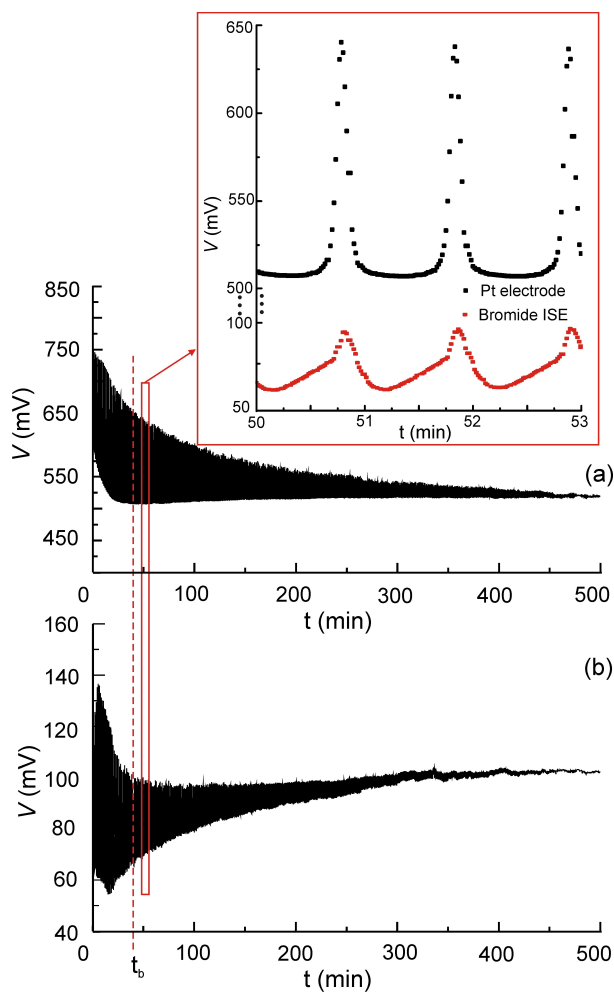


Fig. 1 Temporal trace of oscillations observed in the ruthenium-catalyzed BZ reaction without acetone at the Pt electrode (a) and a bromide selective electrode (b). Initial concentrations: 0.05 M NaBrO₃, 0.20 M malonic acid, 1.0×10^{-4} M Ru(bpy)₃SO₄, and 0.50 M H₂SO₄. The inset shows expanded scale of both potentials. The time interval between data points is 1 s.

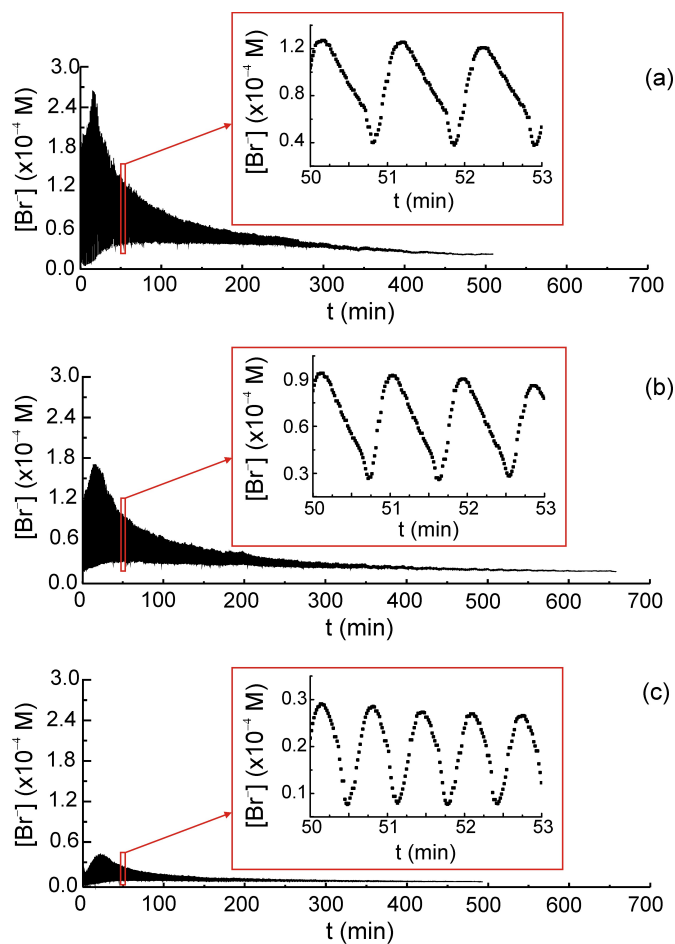


Fig. 2 Effect of acetone concentration on the temporal oscillations of bromide concentration, for (a) 0.00, (b) 0.05, and (c) 0.50 M acetone.

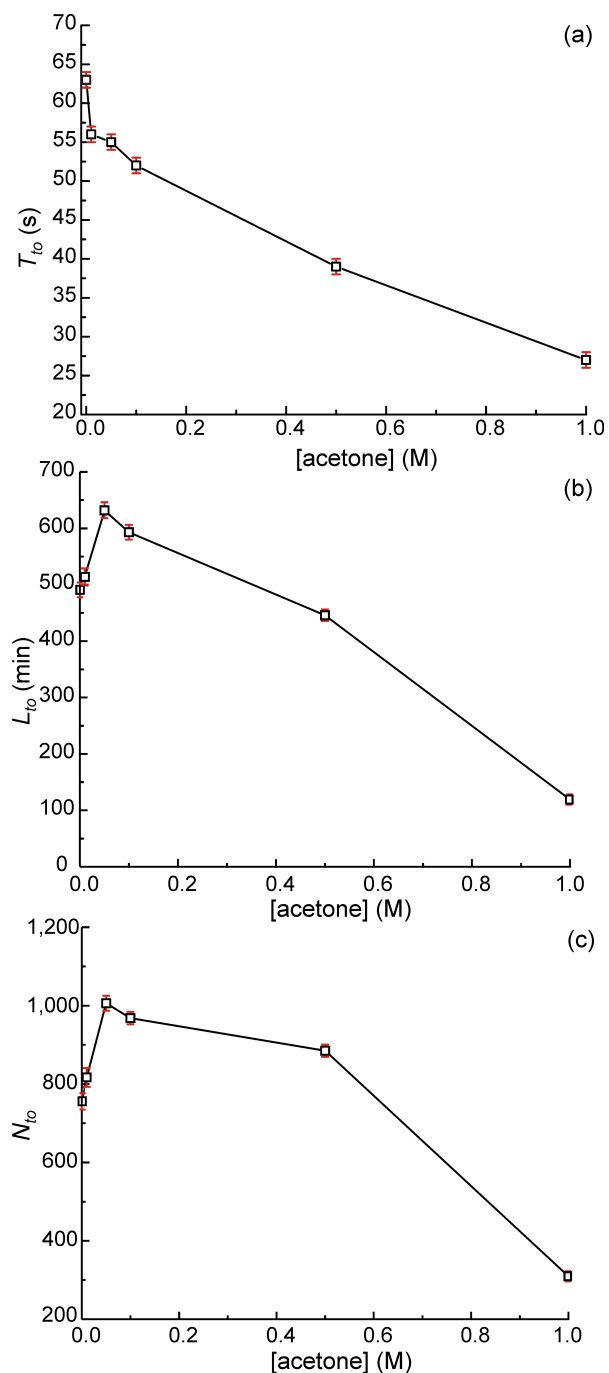


Fig. 3 Effect of acetone on (a) oscillation period T_{to} , (b) oscillation lifetime L_{to} , and (c) oscillation number N_{to} , as a function of acetone concentration. Initial concentrations: 0.05 M NaBrO_3 , 0.20 M malonic acid, 1.0×10^{-4} M $\text{Ru}(\text{bpy})_3\text{SO}_4$, 0.50 M H_2SO_4 . Each data point is mean of 2 experiments.

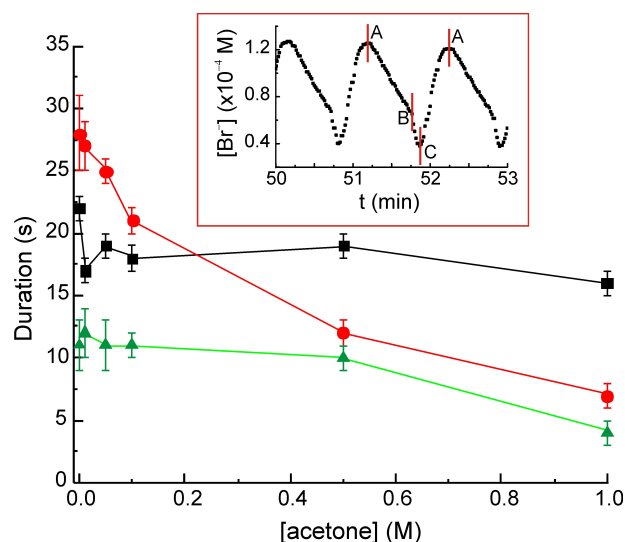


Fig. 4 Effect of acetone on the duration time of the three segments of an oscillation cycle (see inset). The filled circles, filled triangles and filled squares are the times of segment AB, BC and CA, respectively. Each data point is mean of 2 experiments.

mid concentration is shown in Fig. 2. The bromide concentration for each acetone concentration can be calculated from a calibration curve between potential V (in mV) and bromide concentration $[\text{Br}^-]$ (in M) with $V = 51.85 \pm 1.54 \times (\log(1/[\text{Br}^-])) - 131.93 \pm 4.79$ ($r^2 = 0.99$). The amount of bromide significantly decreases with increasing acetone concentration. Figure 2 shows that for 0.05 M acetone the lifetime of the oscillations is the longest. From the insets, one can see that the oscillation period T_{io} decreases with increasing acetone concentration.

Figure 3 is a plot of T_{io} (a), L_{io} (b) and N_{io} (c) as a function of acetone concentration. T_{io} decreases with increasing acetone concentration, steeply at the beginning and becoming linear with increasing concentration. Addition of small amount of acetone (0.01- 0.05 M) to the BZ reaction extends the life-

time of oscillation L_{io} and also increase the number of oscillations N_{io} . However, L_{io} and N_{io} decrease, when the acetone concentration is increased (0.10-1.00 M). From the experimental results in Fig. 3, the longest lifetime of oscillation and the highest number of oscillations is observed for the acetone concentration of 0.05 M.

The effect of acetone on the profile of an oscillation cycle is depicted in Fig. 4. The concentration of Br^- as a function of time for the condition without acetone is used as an example for characterizing the duration of the various processes of a single oscillation (see inset of Fig. 4). The temporal oscillations in one cycle can be divided into 3 processes. The first step (AB) is the decrease of $[\text{Br}^-]$ from level A to level B, at which the concentration of Br^- sharply decreases to level C (step BC), due to the oxidation of the catalyst. Subsequently, Br^- is regenerated and its concentration increases back to level A (step CA). We found that the duration of step AB decreases with increasing acetone concentration, whereas the durations of BC and CA are approximately constant in the range of low acetone concentration, up to 0.50 M.

3.2 Spatio-temporal patterns

In this section, the effect of acetone on the dynamics of waves in the ruthenium-catalyzed BZ reaction is investigated. A summary of spatio-temporal patterns observed under addition of acetone is presented in the series of images in Fig. 5. The wave formation can be qualitatively divided into two types, the predominantly regular (Figs. 5a-5c) and irregular (Figs. 5d-5f) wave patterns. These chemical waves appear spontaneously af-

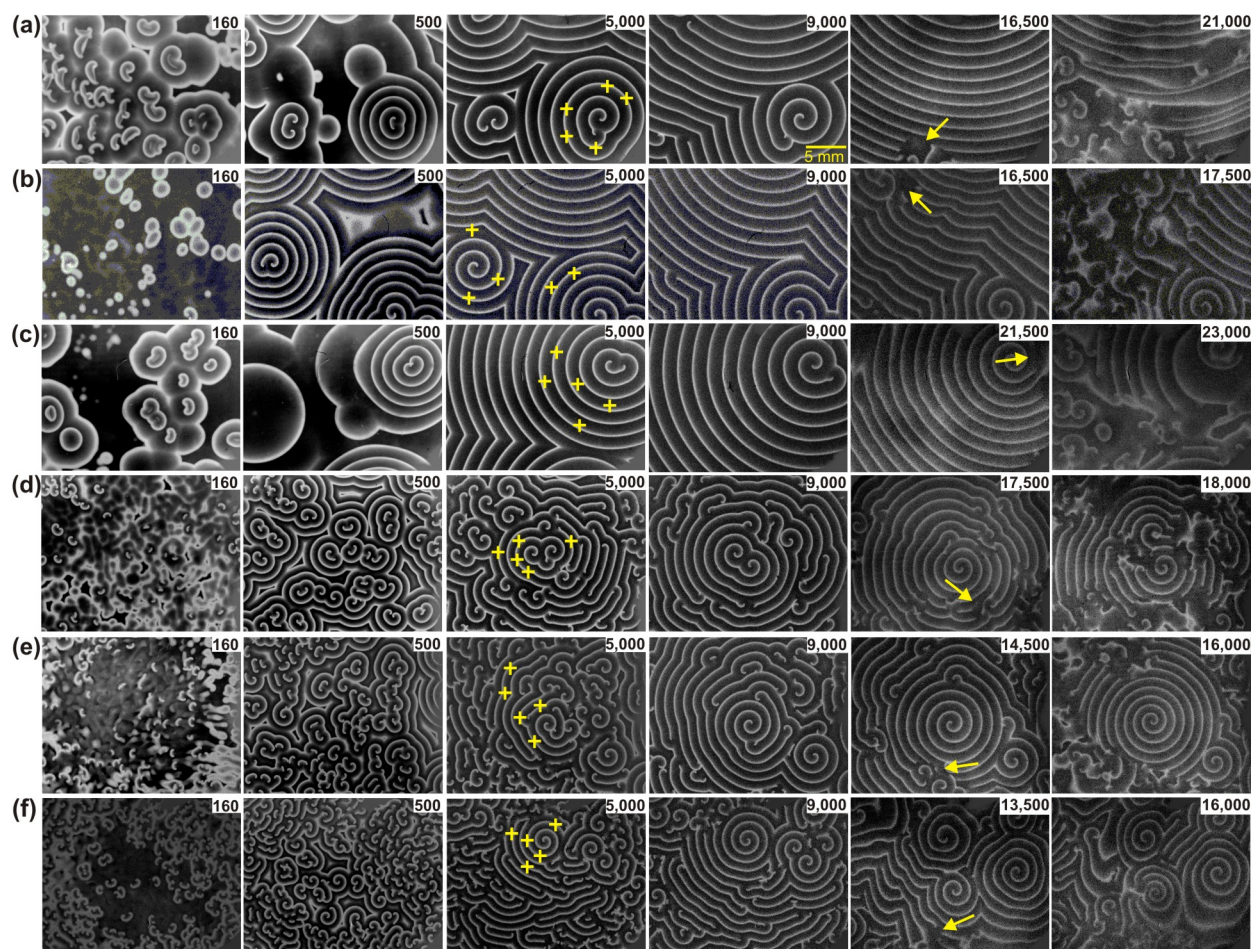


Fig. 5 Spatio-temporal patterns of regular waves (a-c) and irregular waves (d-f) under the variation of acetone concentration: (a) 0.00, (b) 0.01, (c) 0.05, (d) 0.10, (e) 0.50, and (f) 1.00 M. Initial concentrations: 0.05 M NaBrO_3 , 0.20 M malonic acid, 0.50 M H_2SO_4 , 5.0×10^{-4} M $\text{Ru}(\text{bpy})_3\text{SO}_4$. Symbol + indicates the measuring point for period determination. Arrows indicate locations where wave fronts break. Numbers are time in second.

ter pouring the BZ solution on to the gel (see first column of Fig. 5). The oxidation waves of $\text{Ru}(\text{bpy})_3^{3+}$ appear as bright fronts on a dark background. For 0.00 - 0.05 M acetone (Figs. 5a-5c), the target patterns and small wavelets with open ends develop into spiral-shaped waves (see second column). The spiral waves annihilate each other and finally only the higher frequency spiral dominates (third and fourth columns). This rotates until a front breaking occurs at the location indicated by an arrow (fifth column). Such breaks finally invade most of the observation area (sixth column).

With further increase of acetone concentration (0.10-1.00 M), the formation of waves becomes different (see series of images of Figs. 5d-5f) as compared to the previous conditions (0.00-0.05 M). Many small wave segments with open ends develop initially (see first column) to form small rotating spirals and eventually irregular wave patterns consisting of many small spiral waves (see second column). The irregular wave patterns become regular with time, when the higher frequency spirals dominate. Subsequently, the dynamics of wave formation is similar to the first group of wave patterns.

The lifetime of waves (L_{sto}) is defined as the time interval between first appearance of the wave and the aging of wave fronts, which is the time when the area of the front breaking is *ca.* 5 mm². L_{sto} for 0.00, 0.01, 0.05, 0.10, 0.50, and 1.00 M acetone is 268 ± 7 , 276 ± 5 , 346 ± 8 , 260 ± 6 , 235 ± 6 , and 227 ± 6 min, respectively. The longest lifetime was observed, for acetone at the concentration of 0.05 M. This result is consistent with the experimental finding for temporal oscillations (see Sec. 3.1).

The wave period (T_{sto}) is defined as the time between the

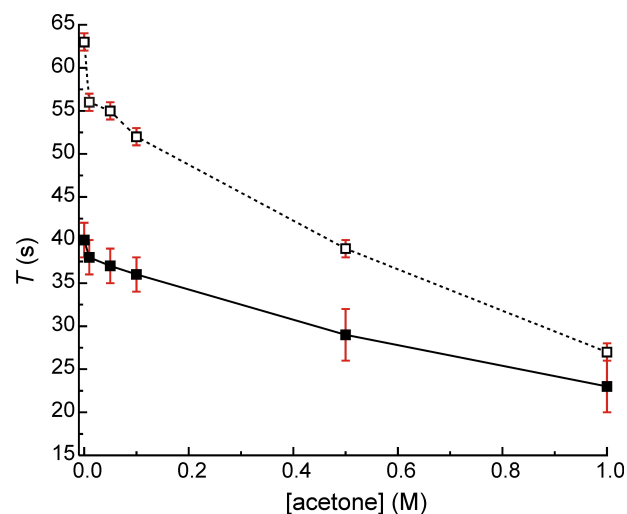


Fig. 6 Comparison between the period of waves T_{sto} (filled squares), and the period of temporal oscillations T_{to} (open squares), as a function of acetone concentration. Each data point is mean of 2 experiments.

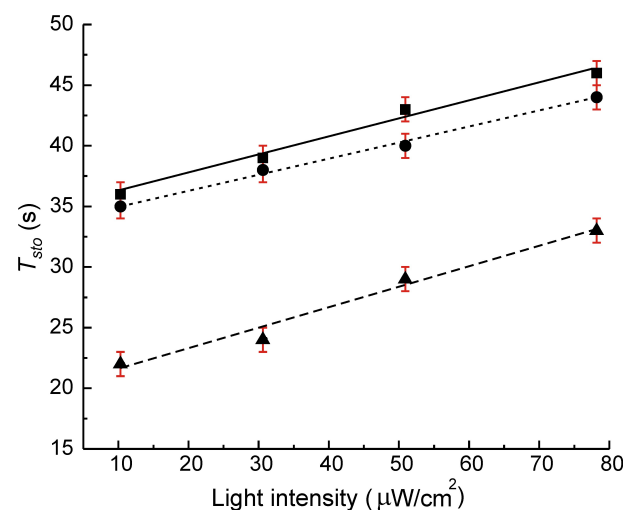


Fig. 7 Wave period T_{sto} in the photosensitive BZ reaction with 0.00 M (filled squares), 0.05 M (filled circles), and 0.50 M acetone (filled triangles). Initial concentrations: 0.05 M NaBrO_3 , 0.20 M malonic acid, 0.50 M H_2SO_4 , 5.0×10^{-4} M $\text{Ru}(\text{bpy})_3\text{SO}_4$, and acetone. Each data point is mean of 2 experiments.

passages of two successive wave fronts passing a preselected measuring point (see crosses in the third column of Fig. 5). It was determined from the mean of 5 measuring points. T_{sto} was evaluated in the time interval 45-55 min, similar to the calculations for temporal oscillations (Sec. 3.1). For example, T_{sto} in Fig. 5a, in time interval 45-55 min, is 40 ± 2 s. The effect of acetone on T_{sto} in comparison with T_{to} is shown in Fig. 6. The period of both waves and temporal oscillations decreases with increasing acetone concentration. However, the period of the waves is much smaller than that of temporal oscillations.

Finally, the photosensitivity of chemical waves was investigated for various acetone concentrations. The variation of T_{sto} with light intensity is shown in Fig. 7. T_{sto} increases linearly with increasing light intensity for all acetone concentrations. The slope of the line is an indicator of the photosensitivity of the system, which is almost the same for all concentrations of acetone. Therefore, the addition of acetone has only a slight influence on the photosensitivity of the system. It may be noted that for a given light intensity, the wave period decreases with the increasing acetone concentration.

4 Discussion

The experimental results are discussed based on three processes of the FKN mechanism: process A—the decrease of Br^- to a critical concentration, the generation and consumption of Br_2 via the bromination reaction; process B—the autocatalytic reaction; and process C—the regeneration of Br^- .¹⁻³ A summary of the effect of acetone on the wave period (T_{sto}) and period of temporal oscillations (T_{to}) is shown in Fig. 6. T_{sto} and

T_{to} significantly decrease with increasing acetone concentration. This can be explained by considering the fact that the increase of acetone concentration decreases the concentration of Br^- (see the decreasing of peaks amplitudes in Fig. 2a-2c). As the amount of Br^- is diminished, the system needs a shorter time to remove Br^- via the process A, and consequently the period is shortened.

The major role of process A in this context is confirmed by the results in Fig. 4, where the acetone effects on the duration of each oscillation process is investigated. The durations for AB, BC, and CA in the inset of Fig. 4 correspond to the durations in the processes A, B, and C of the FKN mechanism, respectively. The oscillation period is the sum of these three time intervals. One sees that increasing the acetone concentration causes a decrease of the duration AB (filled circles in Fig. 4), whereas durations BC (filled triangles) and CA (filled squares) remain quite constant. Apparently, acetone strongly influences and shortens only the time interval AB (process A in the FKN mechanism). The results agree well with previous works.^{8,10}

The corresponding reaction mechanism is proposed according to Table 1. In our system, a mixed organic substrate (malonic acid and acetone) is presented. Therefore, the competitive consumption of Br_2 via the bromination of both malonic acid (R7) and acetone (R10) in process A is involved. The enolization of malonic acid and acetone is represented by R5-R6 and R8-R9, respectively. The bromination reactions occur via the enol form, which is the more favored form for a reaction with Br_2 .²⁰

Table 1 Process A of the FKN mechanism including a mixed organic substrate malonic acid and acetone

		Reaction		Rate constant	Reaction rate	Ref.
R1	$\text{BrO}_3^- + \text{Br}^- + 2\text{H}^+$	\rightarrow	$\text{HBrO}_2 + \text{HOBr}$	$k_1=2.0 \text{ M}^{-3}\text{s}^{-1}$	$k_1[\text{BrO}_3^-][\text{Br}^-][\text{H}^+]^2$	19
R2	$\text{HBrO}_2 + \text{Br}^- + \text{H}^+$	\rightarrow	2HOBr	$k_2=2 \times 10^6 \text{ M}^{-2}\text{s}^{-1}$	$k_2[\text{HBrO}_2][\text{Br}^-][\text{H}^+]$	19
R3	$\text{HOBr} + \text{Br}^- + \text{H}^+$	\rightarrow	$\text{Br}_2 + \text{H}_2\text{O}$	$k_3=2.3 \times 10^9 \text{ M}^{-2}\text{s}^{-1}$	$k_3[\text{HOBr}][\text{Br}^-][\text{H}^+]$	19
R4	$\text{Br}_2 + \text{H}_2\text{O}$	\rightarrow	$\text{HOBr} + \text{Br}^- + \text{H}^+$	$k_4=2.0 \text{ s}^{-1}$	$k_4[\text{Br}_2]$	19
R5	MA	\rightarrow	MA_{ENOL}	$k_5=3 \times 10^{-3} \text{ s}^{-1}$	$k_5[\text{MA}]$	19
R6	MA_{ENOL}	\rightarrow	MA	$k_6=200 \text{ s}^{-1}$	$k_6[\text{MA}_{ENOL}]$	19
R7	$\text{Br}_2 + \text{MA}_{ENOL}$	\rightarrow	$\text{BrMA} + \text{Br}^- + \text{H}^+$	$k_7=1.91 \times 10^6 \text{ M}^{-1}\text{s}^{-1}$	$k_7[\text{Br}_2][\text{MA}_{ENOL}]$	19
R8	$\text{AC} + \text{H}^+$	\rightarrow	$\text{AC}_{ENOL} + \text{H}^+$	$k_8=8.3 \times 10^{-5} \text{ M}^{-1}\text{s}^{-1}$	$k_8[\text{AC}][\text{H}^+]$	10
R9	$\text{AC}_{ENOL} + \text{H}^+$	\rightarrow	$\text{AC} + \text{H}^+$	$k_9=21.3 \text{ M}^{-1}\text{s}^{-1}$	$k_9[\text{AC}_{ENOL}][\text{H}^+]$	10
R10	$\text{Br}_2 + \text{AC}_{ENOL}$	\rightarrow	$\text{BrAC} + \text{Br}^- + \text{H}^+$	$k_{10}=1.03 \times 10^7 \text{ M}^{-1}\text{s}^{-1}$	$k_{10}[\text{Br}_2][\text{AC}_{ENOL}]$	10

Abbreviations: MA \equiv CH₂(COOH)₂, MA_{ENOL} \equiv (HOOC)CH=C(OH)₂, BrMA \equiv BrCH(COOH)₂, AC \equiv CH₃COCH₃, AC_{ENOL} \equiv CH₂=COHCH₃, BrAC \equiv BrCH₂COCH₃

The results in Fig. 3 show that adding a small amount of acetone (0.01-0.05 M) can prolong the lifetime of temporal oscillations (L_{to}) and increase the oscillation number (N_{to}) (increase of L_{to} and N_{to} in Fig. 3b and 3c for $0.01 \text{ M} \leq [\text{acetone}] \leq 0.05 \text{ M}$). In the presence of the competitive consumption of Br_2 it can be expected that the removal of Br_2 (source of inhibitor Br^-) is enhanced and therefore the oscillation lifetime is prolonged. However, this is valid only for a certain range of acetone concentration. Let us consider the effect of acetone on the oscillations as a whole from the results for lifetime L_{to} and oscillation number N_{to} in Fig. 3b and 3c, respectively. Adding a small amount of acetone (0.01-0.05 M) enhances both L_{to} and N_{to} . On the other hand, further increasing the acetone concentration (0.10-1.00 M) results in a decrease of L_{to} and N_{to} . This finding indicates a disadvantage, because adding large amounts of acetone (>0.05 M) makes the system deficient of Br_2 and consequently Br^- to create favorable conditions for oscillations.

It suggests that a balance between the production of Br_2 and its consumption is important to get the longest lifetime of oscillations.

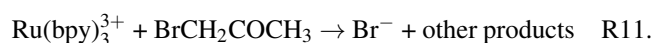
The curves in Fig. 6 indicate that the period of the temporal oscillations T_{to} under stirring (open squares) is longer than the period of the unstirred wave pattern T_{sto} (filled squares) for all acetone concentrations, although their trends are the same. To explain this result, one should focus on the stirring effect, because it constitutes a major difference between temporal oscillations (stirred system) and waves (unstirred system). In an additional study, the effect of the stirring rate on the temporal oscillations in the used recipe excluding acetone was investigated (ESI 1). There is a linear relation between T_{to} (unit of s) and stirring rate (unit of rpm):

$$T_{to} = 0.05 \pm 0.01 * \text{stirring rate} + 45.50 \pm 3.02 \quad (r^2 = 0.94).$$

This relation suggests that T_{to} under the non-stirred conditions equals 45.50 s. The value is close to the unstirred T_{sto} in

the recipe without acetone (40 ± 2 s). Based on this linear relation, at the stirring rate of 300 rpm, which corresponds to the stirring rate in Fig. 6, T_{10} is equal to 60.50 s. This value is consistent with the oscillation period $T_{10} = 63 \pm 1$ s found without acetone (Fig. 6). Therefore, the period of temporal oscillations is larger than that of waves because of the stirring effect. Since the system is physically closed, the produced Br_2 gas, evaporating and accumulating above the BZ solution, can be redissolved into the solution. The redissolving of Br_2 is enhanced by stirring, as shown in supplementary result (EIS 1), where the concentration of inhibitor Br^- increases with increasing stirring rate. It is thus plausible that the concentration of Br^- in the temporal oscillation (stirred) is larger than that of the wave formation (unstirred). Consequently, for temporal oscillation the system takes longer time to remove Br^- via the process A. Therefore, the period T_{10} is larger than T_{sto} .

In this work we have observed irregular patterns in the BZ system, when using high acetone concentrations (0.10-1.00 M), as shown in the second column of Figs. 5d-5f. These irregular patterns may occur due to inhomogeneities in the system.²¹ We suspect that $\text{BrCH}_2\text{COCH}_3$, which is a product from the bromination of acetone and poorly soluble in H_2O (the solvent of the BZ solution), may cause such inhomogeneities in the system. As the produced $\text{BrCH}_2\text{COCH}_3$ is poorly dissolved in H_2O , it forms an emulsion in the BZ solution. It can sink in the BZ solution because its density (1.634 g cm^{-3}) is higher than that of H_2O . Moreover, it can produce Br^- via the reaction shown as follows¹¹:



The BZ solution with variation of acetone concentration was investigated additionally for detecting $\text{BrCH}_2\text{COCH}_3$ in each condition (ESI 2). The $\text{BrCH}_2\text{COCH}_3$ content was detected by using a $^1\text{H-NMR}$ spectrometer. For the BZ solution with a small amount of acetone (0.05 M), no characteristic peak of $\text{BrCH}_2\text{COCH}_3$ is observed. However, peaks appear at 3.90 (ppm, 2H) and 2.38 (ppm, 3H) in case of a large amount of acetone (0.10 and 0.50 M) (see EIS 2). Therefore, $\text{BrCH}_2\text{COCH}_3$ is observed in the BZ solution with high acetone concentration.

When the BZ solution is pipetted onto the catalyst gel surface, $\text{BrCH}_2\text{COCH}_3$ sinks and covers the gel surface. This causes the inhomogeneity on the surface. Moreover, it produces inhibitor Br^- locally via the reaction with $\text{Ru}(\text{bpy})_3^{3+}$ (R11). This may result in the breaking of wave fronts and the occurrence of many small wave segments with open ends. Such wave segments subsequently transform into the irregular wave patterns. However, the detailed mechanism has not been investigated in this work.

As shown in Fig. 7, the wave period (T_{sto}) increases linearly for all acetone concentrations, when the light intensity increases. For the $\text{Ru}(\text{bpy})_3^{2+}$ -catalyzed BZ reaction, the illumination mainly affects the $\text{Ru}(\text{bpy})_3^{2+}$, which leads to the production of Br^- .^{22,23} The amount of Br^- increases with the enhancement of the illumination intensity.²²⁻²⁵ As a result of the increment of Br^- production the system takes a longer time to remove Br^- via the process A. Therefore, T_{sto} increases with increasing of the light intensity. Moreover, the photosensitivity of the system represented by the slopes of the graphs in Fig. 7 is constant for all concentrations of acetone. This suggests that

addition of acetone does not interfere with the photosensitivity of Ru(bpy)₃²⁺-catalyzed BZ reaction.

5 Conclusion

Our experimental results demonstrate that the periods of temporal oscillations and waves are significantly shorter, when the acetone concentration is increased. Our detailed study about the effects of acetone on the duration of each oscillation process shows that acetone is involved in the process A of the FKN mechanism. In this process, the competitive consumption of Br₂ via the bromination of both malonic acid and acetone plays an important role regarding the lifetime of temporal oscillations and waves. Adding small amounts of acetone (removal of inhibitor Br⁻) improves the lifetime. However further increasing the acetone concentration (deficient of Br⁻) results in the decrease of the lifetime. This suggests that a balance between the production of Br₂ and its consumption is important to achieve the longest lifetime of temporal oscillations and waves. The study on the effect of acetone on the photosensitivity of waves in the Ru(bpy)₃²⁺ - catalyzed BZ reaction shows that acetone does not affect the photosensitivity of this system. Therefore, this system should be useful for long term study and control of the wave dynamics by light. The results of the effect of acetone on the wave patterns show that the regular wave patterns are formed for addition of small amount of acetone, whereas irregular ones are observed on adding larger amount of acetone. NMR data suggest that the inhomogeneity on the catalyst gel surface is caused by bromoacetone which is responsible for the breakup of the chemical wave fronts, resulting in the occur-

rence of the irregular wave patterns.

6 Acknowledgement

We thank Wannabhorn Motina for her assistance in calibrating the bromide selective electrode. This work was financially supported by the Office of the Higher Education Commission under the Strategic Scholarships for Frontier Research Network for the Ph.D. Program, Thai Doctoral degree.

References

- 1 R. J. Field, E. Körös, R. M. Noyes, *J. Am. Chem. Soc.*, 1972, **94**, 1394-1395.
- 2 R. J. Field, E. Körös, R. M. Noyes, *J. Am. Chem. Soc.*, 1972, **94**, 8649-8664.
- 3 R. J. Field, R. M. Noyes, *J. Am. Chem. Soc.*, 1974, **96**, 2001-2006.
- 4 I. R. Epstein and J. A. Pojman, An introduction to nonlinear chemical dynamics "Oscillations, waves, patterns, and chaos", Oxford university press, New York, 1998.
- 5 S. K. Scott, Oscillations, Waves, and Chaos in Chemical Kinetics, Oxford University Press, New York, 1994.
- 6 M. Menzinger and P. Jankowsky, *J. Phys. Chem.*, 1990, **94**, 4123-4126.
- 7 I. Berenstein, J. Ágreda, D. Barragán, *Phys. Chem. Chem. Phys.*, 1999, **1**, 4601-4603.
- 8 I. Berenstein, J. Ágreda, D. Barragán, *J. Phys. Chem.*, 1999, **103**, 9780-9782.

- 9 I. Berenstein, D. Barragán, *J. Braz. Chem. Soc.*, 2004, **15**, 844-848.
- 10 R. J. Field, P. M. Boyd, *J. Phys. Chem.*, 1985, **89**, 3707-3714.
- 11 I. Szalai, K. Kurin-Csörgei, V. Horváth, M. Orbán, *J. Phys. Chem. A*, 2006, **110**, 6067-6072.
- 12 M. Orbán, K. Kurin-Csörgei, A. M. Zhabotinsky, I. R. Epstein, *Faraday Discuss.*, 2001, **120**, 11-19.
- 13 O. Kheowan, Dynamics of spiral waves under feedback control in the light-sensitive Belousov-Zhabotinsky reaction, Ph.D. Thesis, 2001.
- 14 O. Kheowan, V. Gáspár, V. S. Zykov, S. C. Müller, *Phys. Chem. Chem. Phys.*, 2001, **3**, 4747-4752.
- 15 W. W. Nazaroff and L. Alvarez-Cohen, *Environmental Engineering Science*, John Wiley, New York, 2001.
- 16 S. S. Jacobs, I. R. Epstein, *J. Am. Chem. Soc.*, 1976, **98**, 1721-1724.
- 17 J. Wang, K. Yadav, B. Zhao, Q. Y. Gao, D. S. Huh, *J. Chem. Phys.*, 2004, **121**, 10138-10144.
- 18 T. Yamaguchi, L. Kuhnert, Zs. Nagy-Ungvarai, S. C. Müller, B. Hess, *J. Phys. Chem.*, 1991, **95**, 5831-5837.
- 19 L. Györgyi, T. Turányi, R. J. Field, *J. Phys. Chem.*, 1990, **94**, 7162-7170.
- 20 A. Sirimungkala, H. D. Fösterling, V. Dlask, R. J. Field, *J. Phys. Chem.*, 1999, **103**, 1038-1043.
- 21 J. Maselko, J. S. Reckley, K. Showalter, *J. Phys. Chem.*, 1989, **93**, 2774-2780.
- 22 M. Jinguji, M. Ishihara, T. Nakasawa, *J. Phys. Chem.*, 1992, **96**, 4279-4281.
- 23 L. Kuhnert, *Nature*, 1986, **319**, 393-394.
- 24 M. K. Ram Reddy, Z. Szláivik, Zs. Nagy-Ungvarai, S. C. Müller, *J. Phys. Chem.*, 1995, **99**, 15081-15085.
- 25 S. Kádár, T. Amemiya, K. Showalter, *J. Phys. Chem.*, 1997, **101**, 8200-8206.